IOP Publishing Journal of Micromechanics and Microengineering
J. Micromech. Microeng. **00** (2015) 000000 (7pp) UNCORRECTED PROOF

Bending waveguides made in x-cut lithium niobate crystal for technological applications

V Guarepi[1], C Perrone[1,2], M Aveni[1], F Videla[1,3] and GA Torchia[1,2]

[1] Centro de Investigaciones Ópticas (CIOp) CONICET La Plata-CICBA, Camino Centenario y 506, M.B. Gonnet (1897), Provincia de Buenos Aires, Argentina
[2] Departamento de Ciencia y Tecnología, Universidad Nacional de Quilmes, B1876BXD Bernal, Buenos Aires, Argentina
[3] Facultad de Ingeniería, Universidad Nacional de la Plata, Depto de Ciencias Básicas, 1900 La Plata, Buenos Aires, Argentina

AQ1 E-mail: xxxx

Received 25 July 2015, revised 2 October 2015
Accepted for publication 6 October 2015
Published

Abstract

In this paper we analyse the performance of several designs of integrated optical deviators made in x-cut lithium niobate crystals by means of femtosecond laser writing using the double line approach. Straight and bent guiding structures have been designed and implemented by using this technique. Well-confined propagation modes at communications wavelengths (1.55 μm) were conducted in these structures with acceptable overall losses (less than 2 dB cm^{-1}). Further, a discussion about the optical propagation losses for curved and straight deviators devices is included in this work. At a low aperture angle (less than 0.2°), as expected, low losses were determined for both structures; however, a weak output light was observed for large angles (greater than 0.2°) in the straight optical circuits. In contrast, a smooth variation of the output was measured for the bent structures. The results presented in this paper support the actual possibility of the technological implementation of integrated optical circuits for optical communications fabricated with ultrashort laser writing in lithium niobate crystals. In addition, some hypotheses of loss mechanisms that are normally not considered are discussed in order to explain the differences between the measured values and predictions obtained calculating with the usual models.

Keywords: femtosecond laser writing, integrated optical deviators, curved guiding structures, propagation losses

AQ2 (Some figures may appear in colour only in the online journal)

1. Introduction

Currently the integrated photonic represents a key sector able to support the real levels of information and data transmission demanded from optical communications data, video and imaging processing systems. To cover these technological necessities, there are several integrated optical elements that are currently being used in these fields i.e. directional couplers in optical amplifiers, ring resonators as filters for optical communications, and also as angular rate sensors for aerospace systems, among others [1–3]. Standard and well-established waveguide fabrication methods are commonly used for obtaining these optical circuits e.g. proton exchange, metal in-diffusion, ion implantation, [4–6]. To optimise these fabrication processes, for instance the guiding structures should have low propagation losses and guide a single mode light in the communications wavelength region [7–9]. In order to establish any fabrication waveguide technique as a new acceptable technology it is necessary to carry out many experiments, characterisations, models, procedures, prototypes etc. In this sense, the ultrashort laser writing technique started to

JNL:JMM PIPS: AA05E2 TYPE: PAP TS: NEWGEN DATE:21/10/15 EDITOR: JW SPELLING: US

appear more than ten years ago when the chirped pulse amplifier (CPA) systems were developed. Ultrashort laser writing has been usefully employed in several optical materials and many suitable devices have been conducted for integrated photonics applications which are based in guiding structures made with different writing approaches. Among the optical devices implemented by this method during recent years, we can point out the following: integrated laser, optical amplifiers, sensors, optical circuits, non-linear devices, Mach Zehnder interferometers, Y branch, directional couplers etc [3]. As is well known, femtosecond laser writing is a wide processing technique to fabricate integrated optical circuits by a one-step process and low cost, which can be applied to many optical materials [10]. By means of non-linear processes such as multi photon and avalanche absorption, ultrashort laser interaction gives rise to tightly modified regions. These zones, located either at the focal or beside the laser track depending on the pulse energies, constitute the optical waveguide structure. The first waveguide group corresponds to the so-called Type I waveguides. On the other hand, for higher energies, getting power about the optical breakdown threshold for the material, Type II waveguides are constructed. An other interesting development was the depressed cladding waveguides in LiNbO3 [11, 12], also called Type III. The most important goal from this technique is the three-dimensional tailoring which boosts its applicability to many integrated photonics targets [13–17], see also [18] for Type I 3D waveguides. The lithium niobate (LiNbO3) crystal has many interesting optical properties such as excellent non-linear, electro-optic, piezo-optic coefficients and it is also broadly used for technological purposes, i.e. as an integrated phase modulator working up to 100 Gbit s^{-1} for optical transmission data [19, 20]. Some pioneering works have been reported related to femtosecond laser writing in lithium niobate, i.e. [21–23]. In order to design any new integrated optical circuits it is very important to consider the bending losses which are a key point to control the propagation losses for these kinds of integrated devices. In this sense, considering low-contrast waveguides as those guiding structures with a refractive index increment of about 10^{-3}, large radii should be proposed to limit the bending losses. As a consequence curved waveguides above 10 mm radii have been considered in our work [24, 25]. In this work, we have fabricated curved and straight deviators integrated in x-cut lithium niobate samples 25 mm in length by means of femtosecond laser writing. The overall propagation losses for both devices have been determined by measuring the output power related to the input power for each system. Complementarily, in order to compare the experimental data, computational simulations based in the beam propagation method (BPM) have been performed by using the commercial software RSoft* [26, 27]. We have studied the integrated deviators considering different aperture angles, from 0.2° to 1° for the straight and curved designs conducted in this work.

2. Materials and procedures

2.1. Writing procedure

In this work, the integrated deviators were fabricated in 3″ wafer of x-cut LiNbO3 crystal from Laser Technology Inc. (USA). The waveguide structures were generated using a Chirped Pulse Amplification (CPA) system lasing at 796 nm based in a Ti:Sapphire ultrafast laser. The system can deliver pulses of 120 fs, a repetition rate of 1 kHz and up to 1 mJ of pulse energy. To record the laser tracks a 20 × (NA = 0.4) microscope objective was used to focus the laser 200 μm below the crystal surface. A writing speed of 25 μm s^{-1} along the *y*-direction, normal to the propagation direction, and 0.7 mJ per pulse were set to record the optical deviators. The width of the waveguides was chosen to be 21 μm; this value was supported by means of computational simulations that guarantee single-mode propagation at 1.55 nm. The optical circuit layout was performed by using a code developed in Visual Basic. This software controls a mechanical system and allows curved waveguides to be performed as well as ordinary straight guiding structures. The motorised x, y, z station consists of three coupled Newport continuous translators with an accuracy of about 0.1 μm and the 25 mm travel each. The deviators were designed tracing two segments of straight waveguides of 3 mm = D1 = D3 in length for the input and the output, respectively. In the middle part of the deviators, curved and straight aperture angles were achieved, as detailed in figure 1.

The angle span was from 0.2° to 1°. Connecting input and output segments a straight waveguide diagonal oriented structure a of 18 mm $(D4^2 + D2^2)^2$ length for each angle was recorded. Otherwise, for the bend structure, smooth curved waveguides were written by means of the software control of the continuous x, y motorised station. The whole length from these constructed structures was 25 mm. Figure 1(a) sketches the main details corresponding to the two types of deviator constructed in this work. Figure 1(b) shows an optical microscope picture, where the beginning of the curved part from the deviator is detailed. After writing the guiding structures into the x-cut lithium niobate samples, the end edges were polished up to optical grade by using a natural diamond powder paste with diameters from 15 μm to 0.25 μm.

2.2. Simulation performance

In order to simulate the optical propagation along the integrated optical deviators defined between two curved and straight type II waveguides (see figure 1(a)), the method known as BPM was performed. This approach uses the paraxial approximation to simplify the scalar Helmholtz equation, which solves the paraxial or Fresnel equation. As is well known, this method assumes that the envelope of the field varies slowly in the direction of propagation (SVEA) [8, 28]. The simulations were performed using the RSoft commercial software [17], in particular by using the tool called BeamProp, which is based on the BPM technique. RSoft uses finite differences with the well-known Crank–Nicholson method to propagate the light into our guiding structures. The boundary conditions commonly imposed at the borders of the simulation window are known as transparent boundary conditions [8, 26, 28]. Straight and curved deviators have been simulated with this software, where the aperture angles from 0.2° to 1° were considered as an input parameter for our studies.

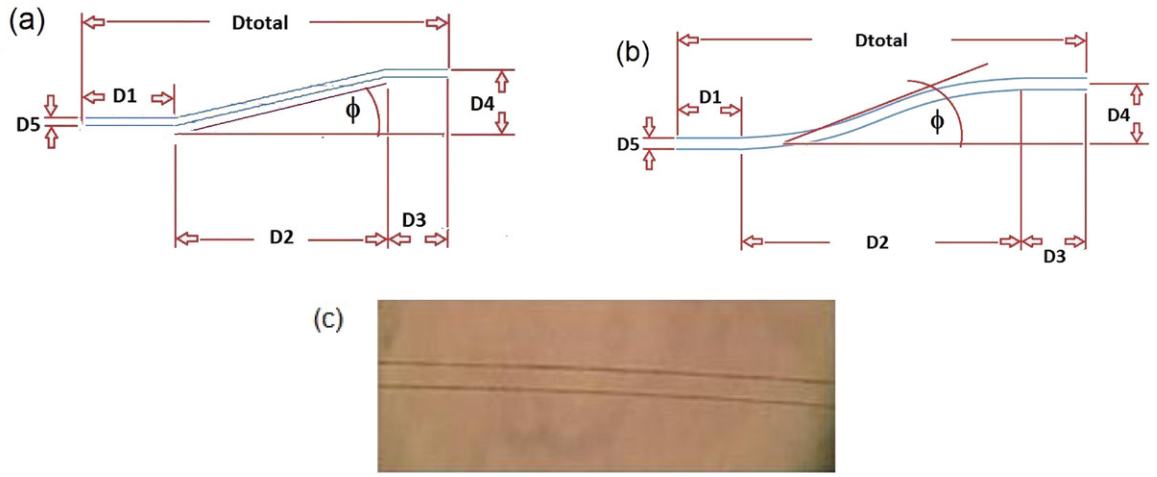

Figure 1. Scheme corresponding to the straight (a) and curved (b) designs for the deviators used in this work. The dimensions and other design parameters are indicated in the picture. (c) Optical image corresponding to the curved part from the deviators constructed in this work in lithium niobate substrates. This image details the laser track used to fabricate the curved structure. The indicated measures are Dt total waveguide length, D1, D3 input and output length of the waveguide, D4 vertical distance between the input and output centre of the wavelength, D2 horizontal length between the input and output, D5 width guide.

2.3. Optical wave guiding characterisation

An exploration of the optical propagation performance of the deviators was carried out in this work; we used a typical end fire coupling system, as described in reference [27]. This setup is formed by naked fiber optics at the input and a microscope objective at the output. The output light from the waveguide structures is focused to the beam profile analyser (Newport LBP2). The coupling light comes from a red and a Distributed Feedback (DFB) diode laser tuned at telecommunications wavelengths (1.55 μm). In addition, a calibrated power meter (Newport 918D series) was used to measure the light power at the input and output from the deviators in order to test the overall losses for these systems.

2.4. Results and discussion

First, an optical characterisation of the integrated deviators was made in this work into lithium niobate samples. For this purpose, a visible laser light at 650 nm at 24 μW was coupled by using a fiber optical end fire system. The amorphisation degree of the crystal lattice induced structural modification, raising the refractive index relative to the surrounding material allowing good performance only in the TM mode. Otherwise, in type II waveguides fabricated in lithium niobate, the TE propagating modes are weakly guided, as is well described in the paper written by M.R. Tejerina *et al* [17]. In this work, the authors considered an elastic model to describe the polarisation properties in the resultant written guiding structure in an x-cut sample.

Multi-mode propagation was observed in all the devices under consideration so single-mode infrared propagation could be reached in these guiding structures. Figure 2 shows a representative guided mode at 1.55 μm from the deviators fabricated in this work. As can be seen, well-confined light at telecommunication wavelength (1.55 μm) is observed. A similar behaviour was tested for the all-integrated optical deviators studied in this paper. On the other hand, for deviators with an aperture angle greater than 0.8° an important reduction in the guided light was observed at the output for both structures (see figure 2(b)).

In order to compare the experimental measurements, we also present simulated results obtained by using the BPM tool from RSoft software [26]. It must be mentioned that a 1 dB cm^{-1} loss in the propagation pathway was added in the simulation program in order to reproduce more real conditions. Figure 3 shows a top view corresponding to energy propagation for a straight (a) and curved (b) deviator with 0.2° and 0.8° degrees of aperture. As can be seen, for an aperture angle of 0.2° there is no evidence of important changes in the guided light for either structure, which means that the deviators have a good performance independently if they are constructed with curved or straight guiding structures. In contrast, for the case of deviators constructed with a 0.8° degree of aperture angle, the coupled light corresponding to the straight deviator (left) shows important intensity variation, which can be associated with the abrupt modification of the guiding structure as it was designed (see figure 1). In these regions the modes show an unstable mode solution until reaching a stable one. This situation occurs two times along the deviators, so this effect is well noticeable where the direction for the guiding structure is markedly changed. In contrast, for curved deviators the coupled mode shows lower losses of intensity due to the smooth change in the guiding direction according to the way these optical circuits were designed.

Complementarily, it was necesary to quantify the overall losses from the simulated deviators, the output power from each device was simulated, as shown in figure 4. This figure shows both straight and curved deviators covering a range from 0.2° to 1° of aperture angle. In the case of the curved ones a small change is observed (less than 5%) between the power launched and the power at the output for the entire range of aperture angles; only after 1.5 mm in length do the differences seem to be important. In contrast, for the straight ones it can be seen

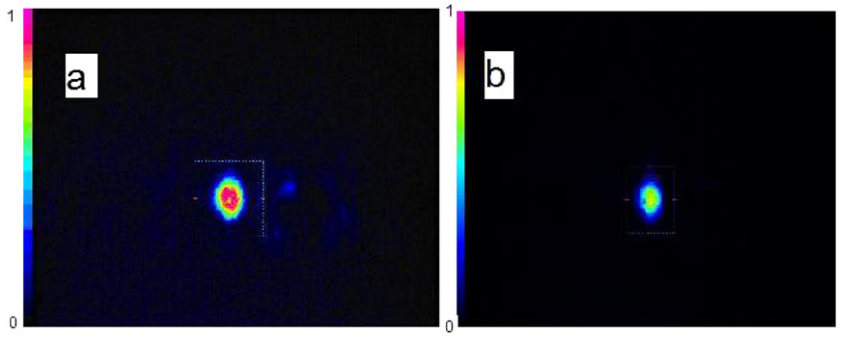

Figure 2. Propagated modes at optical communication wavelengths (1.55 μm) for the deviators constructed with a 0.6° aperture angle for curved (a) and straight guiding structures (b).

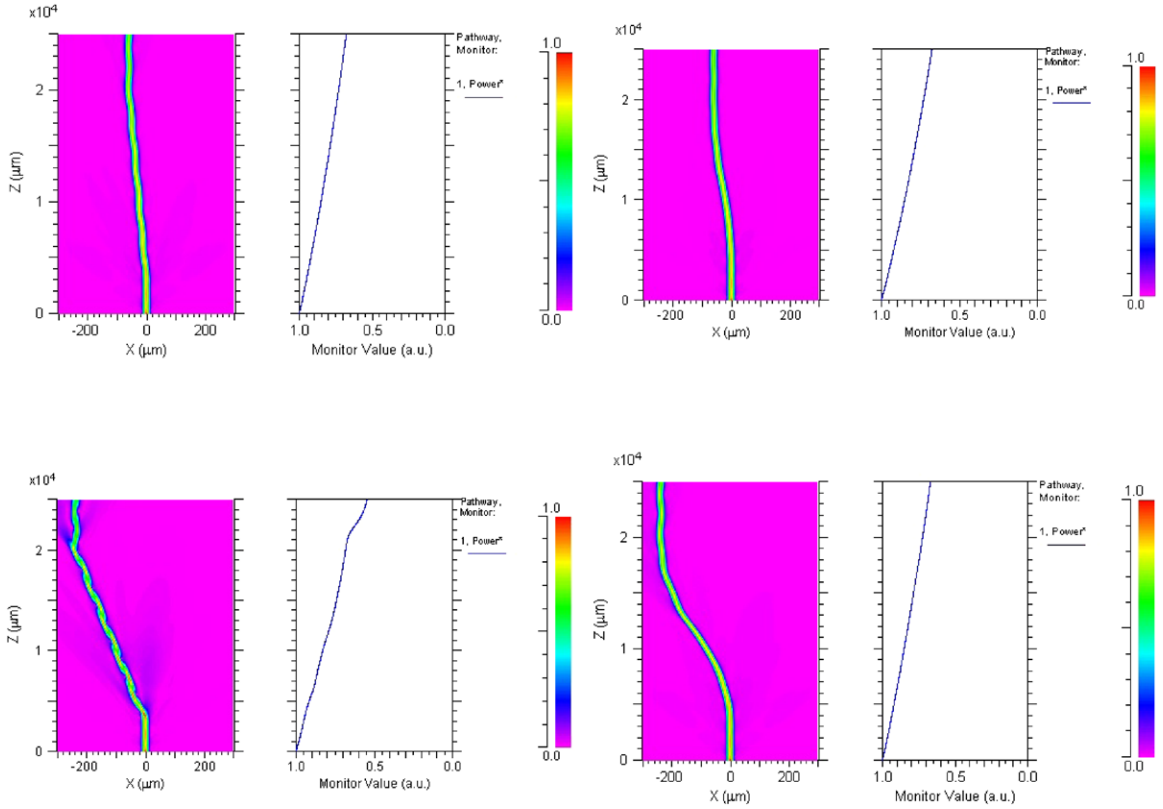

Figure 3. In the first row RSoft monitor window corresponding to straight and curved deviators, both with an aperture angle of 0.2°; at the right-hand side of each one the normalised intensity versus length. The second row is similar to the first row, changing only the aperture angle of each deviator, 0.8° in this case.

that there exist important differences between the amount of power carried to the output for each device as the aperture angle grows in the same range. The straight guiding structures lose up to 50%. Not only is the losses control relevant. In this sense we can also remark, from a technological point of view, that the straight guiding structure could be a more suitable device, considering that the curved structure is time consuming to manufacture if the method used is a standard femtosecond micromachining system. However, considering large aperture angles (>0.8°) there are remarkable differences between straight and curved deviators when the losses are compared. As the angles increase, the losses are larger for straight structures; in consequence, the straight deviators could have an unacceptable performance for aperture angles beyond 0.2°.

To characterise the optical performance of the deviators, the optical losses have been experimentally explored. First, to test the coupling losses corresponding to the experimental procedure used in our work, we have measured it as follows: first of all the total power coming from pigtail fiber from a red laser diode (650 nm in wavelength) was measured; after that, light was coupled into a straight waveguide and then the power at the output was measured. We have estimated coupling losses for our experimental setup with a value of 14 dB and with an uncertainty of $\pm$1 dB. This uncertainty was determined by a statistic measurement of coupling the laser light to the guiding structure. The repeated measurements performed in each deviator (about 30) have allowed us to obtain an uncertainty interval represented as bars in figure 5(a).

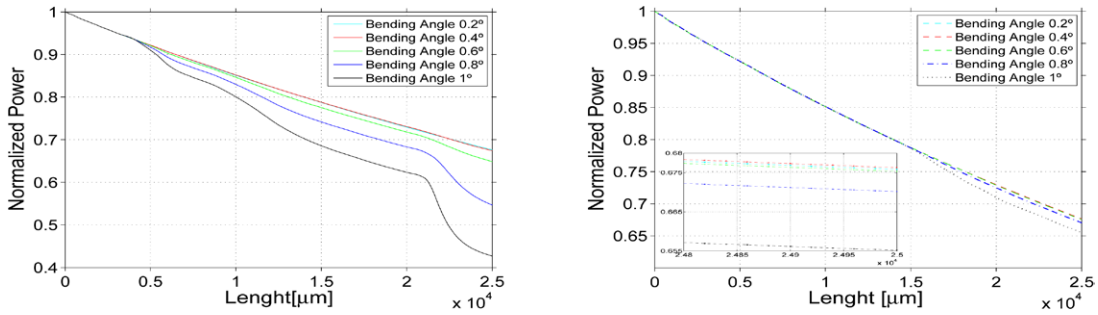

Figure 4. Total output power for both deviators simulated in this paper: straight (left) and curved (right).The range of aperture angles in both cases span from 0.2° to 0.8.

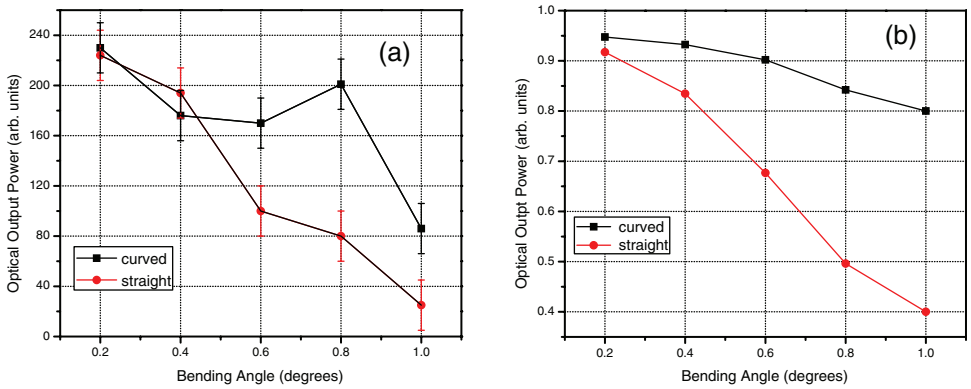

Figure 5. (a) Experimental measurement of losses. The results correspond to the output intensity versus aperture angle for both straight and curved deviators. Also, the error bars are showed for each case; these bars represent the degree of fluctuation in the coupled power in the experiment. (b) Computational simulations of the same losses made with RSoft software. The lines' joining points are only indicative of the trend.

Second, we have started to characterise the deviators by using a IR diode laser light. In this sense, as mentioned above, we first measured the input power before coupling it to the deviators. Figure 5(a) shows the experimental values obtained for the output power as a function of the aperture angle of the deviators, the full rectangles and open circles corresponding to curved and straight deviators, respectively. As can be seen from this picture we can point out two very interesting results: (1) considering the aperture angle of 0.2° for both cases, the overall losses experimentally determined take values of around 2 dB cm^{-1}. This fact is in agreement with the previous results shown in figure 4 for the simulations. Another important issue is the fabrication time spent on writing bend structures with our machining station. Drawing each point that constitutes the curved waveguide is a time-consuming process due to the strategy of writing used in our motorised station. So, for small aperture angles, the losses being very similar, it is more recommended to perform a straight deviator instead of a curved one. As a consequence, using straight optical circuits with a low aperture angle it is possible to increase the rate of production of integrate deviators, which is an important aspect considering the technological requirements in industries because, as shown above, both geometries, curved and straight, have a similar performance. (2) On the other hand, the curved deviators shows a smooth increment of the overall losses as a function of the aperture angle (above 0.2°). This fact can be easily understood considering the gradual growth of bent losses, taking into account the radii defined for each structure at different aperture angles of the deviators. Comparing losses, the advantage of making curved deviators over the straight ones for aperture angles larger than 0.2° is clear.

Finally, to allow a comparison between the experimentally measured values and the results analysis, computational simulations were included in figure 5(b) in the same format as was shown in section (a). The rectangles and circles represent the simulated output power from the curved and straight deviators, respectively. The power values were normalised against the maximum output power value obtained at the 0.2° deviator in both cases. As can be seen, the curved and straight deviators present the same qualitative behaviour considering the dependence of the output power with respect to the aperture angle, as was reported by Hutchenson *et al* [29]. In this work it was demonstrated that the bending losses depend on the arc longitude of each curve of the deviator. On one hand, considering the curved deviators, the losses grow because of the large deviation angles, the arcs are increased as the radii increase. On the other hand, for straight deviators the losses are expected to be larger, as can be seen from Hutcheson's work [29], where to define deviators by using straight segments abrupt changes of angles are considered.

Finally, comparing the simulated results with the experimental data from curved deviators, an important discrepancy can be appreciated related to the overall losses, especially at large aperture or deflection angles. In order to justify why losses are more pronounced, we perform a series of

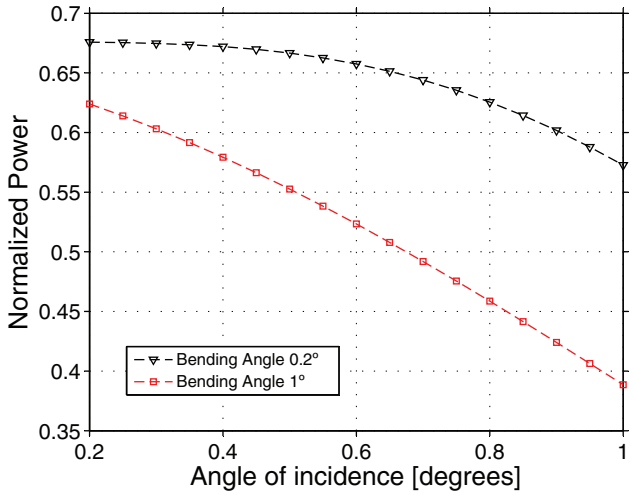

Figure 6. Simulated output power versus the incidence angle for 0.2°(black) and 1°(red) curved deviators, respectively.

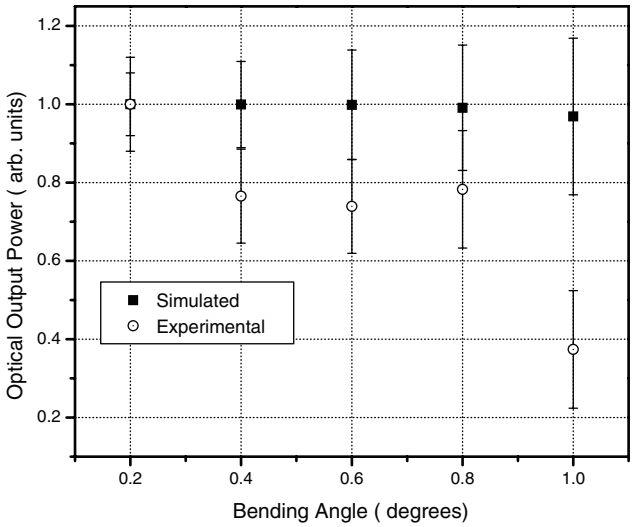

Figure 7. Comparison between experimental measurements and simulated output power versus the incidence angle from 0.2°(black) to 0.8°(red) for curved deviators, respectively.

simulations varying the incident coupling angle for two cases. Figure 6 shows the results of the above-mentioned simulations; as can be seen, they correspond to curved deviators with 0.2° and l° deflection angles, respectively. As the angle of incidence increases, the greater the losses. Both deviators present a similar qualitative behaviour, but the losses are notably larger when comparing between the two cases, i.e. for 0.5° of incident angle; in the case of 0.2° the losses are few (less than 1% of the initial value), while for the case of a 1 degree deviator, the power goes down by approximately half.

Considering the previous analysis on the latter results we can point out that the coupling error (dispersion of the incident angle) has an important effect on the throughput of large aperture deviators. We present in figure 7 a comparison between the experimental and simulated output power for curved deviators considering the angular dispersion, which is unavoidable in our experimental setup. We have represented the measured values and their corresponding error bars, showing an overlap in some cases, although when the aperture angle increases. The error bars in the case of the simulation was calculated by means of R soft software. The rest of the differences can be explained, in particular for the case of large angles, due to the scattering (as was considered in the experimental section) produced by the inhomogeneities present in the fabrication process. This can be understood because large angles of deviation increase the effect of spread light in directions out of the waveguides.

In spite of including this consideration in figure 7, it still shows a little difference between the experimental and simulated results. This discrepancy can be attributed to several other loss mechanisms such as optical absorption, scattering, reflection, numerical aperture etc which are not considered in the propagation software. To diminish these harmful effects, we propose to augment the density of points in the strategy of writing the waveguide.

2.5. Conclusion

In this paper we present experimental results that allow us to consider femtosecond laser writing as a new yet well-established technology for integrated optical circuit fabrication. We demonstrate this statement by constructing optical deviators considering curved and straight guiding structures. In this study, devices designated with aperture angles in the range of 0.2° to 1° were explored. For small aperture angles, the straight and curved devices have shown similar overall losses around of 2 dB cm^{-1}, so this value allows the development of new integrated circuits with reasonable performance and a faster procedure in order to satisfy manufacturing requirements to implement deviators and other splitting devices using straight waveguides. On the other hand, computational simulations based in BPM showed good agreement with the experimental data. In this analysis the overall losses as a function of the aperture and the coupling angles for both strategies of writing were taken into account. The studies carried out in this paper give rise to the consideration of femtosecond laser writing as a versatile technique from various points of view, i.e. (1) It has allowed us to test several geometries with high accuracy in the layout of the tracks. (2) To explore the speed for the implementation of the whole device. (3) The devices manufactured have allowed the measurement of the power relationship input–output (throughput) using standard methods. In summary, femtosecond laser writing is a robust technique for technological purposes.

References

AQ3

[1] Rabus D 2007 *Integrated Ring Resonators, The Compendium (Springer Series in Optical Science)* (Berlin: Springer)
[2] Osellame R, Cerullo G and Ramponi R(ed) 2012 *Femtosecond Laser Micromachining (Topics in Applied Physics)* (Berlin: Springer)
[3] Sugioka K and Cheng Y 2014 Ultrafast lasers–reliable tools for advanced materials processing *Light: Sci. Appl.* **3** e149
[4] Kip D 1998 Photorefractive waveguides in oxide crystals: fabrication, properties, and applications *Appl. Phys.* B **1** 131–50
[5] Sohler W *et al* 2008 Integrated optical devices in lithium niobate *Opt. Photonics News* **19** 24

[6] Chen F 2009 Photonic guiding structures in lithium niobate crystals produced by energetic ion beams *J. Appl. Phys.* **106** 081101
[7] Marowsky G 2014 *Planar Waveguides and other Confined Geometries: Theory, Technology, Production, and Novel Applications* (Berlin: Springer)
[8] Lifante G 2005 *Integrated Photonics: Fundamentals* (New York: Wiley)
[9] Davis K M, Miura K, Sugimoto N and Hirao K 1996 Writing waveguides in glass with a femtosecond laser *Opt. Lett.* **21** 1729
[10] Chen F and Vazquez J R 2014 Optical waveguides in crystalline dielectric materials produced by femtosecond-laser micromachining *Laser Photonics Rev.* **8** 251–75
[11] He R, An Q, Jia Y, Castillo-Vega G R, de Aldana J R V and Chen F 2013 Femtosecond laser micromachining of lithium niobate depressed cladding waveguides *Opt. Mater. Express* **3** 1378–84
[12] Kroesen S, Horn W, Imbrock J and Denz C 2014 Electro–optical tunable waveguide embedded multiscan Bragg gratings in lithium niobate by direct femtosecond laser writing *Opt. Express* **22** 23339–48
[13] Nolte S, Will M, Burghoff J and Tünnermann A 2013 Femtosecond waveguide writing: a new avenue to three-dimensional integrated optics *Appl. Phys.* A **77** 109–11
[14] Florea C and Winick K A 2003 Fabrication and characterization of photonic devices directly written in glass using femtosecond laser pulses *J. Lightwave Technol.* **21** 246–53
[15] Burghoff J, Hartung H, Nolte S and Tünnermann A 2006 Structural properties of femtosecond laser-induced modifications in LiNbO3 *Appl. Phys.* A **86** 165–70
[16] Rodenas A, Maestro L M, Ramirez M O, Torchia G A, Roso L, Chen F and Jaque D 2009 Anisotropic lattice changes in femtosecond laser inscribed Nd3:MgO:LiNbO3 optical waveguides *J. Appl. Phys.* **106** 013110
[17] Tejerina M R, Biasetti D A and Torchia G A 2015 Polarization behaviour of femtosecond laser written waveguides in lithium niobate *Optical Materials* vol 47 (Amsterdam: Elsevier) pp 34–8
[18] Lv J, Cheng Y, Yuan W and Chen F 2015 Three-dimensional femtosecond laser fabrication of waveguide beam splitters in LiNbO3 crystal *Opt. Mater. Express* **5** 1274–80
[19] Kaminow I P, Li T and Willner A E(ed) 2008 *Optical Fiber Telecommunication, Component and Subsystems* A (Amsterdam: Elsevier)
[20] Tomeno I, Matsumura S and Florea C 2002 *Properties of Lithium Niobate* ed K K Wong (London: INSPEC/Institution of Electrical Engineers) p 57 (chapters 4.1 and 4.2)
[21] Gui L, Xu B and Chong T C 2004 Microstructure in lithium niobate by use of focused femtosecond laser pulses *IEEE Photon. Technol. Lett.* **16** 1337–9
[22] Thomson R R *et al* 2006 Optical waveguide fabrication in z-cut lithium niobate (LiNbO3) using femtosecond pulses in the low repetition rate regime *Appl. Phys. Lett.* **88.11** 111109
[23] Nejadmalayeri A H and Herman P R 2006 Ultrafast laser waveguide writing: lithium niobate and the role of circular polarization and picosecond pulse width *Opt. lett.* **31.20** 2987–9
[24] Vannahme C, Suche H, Reza S, Ricken R, Quirino V and Solher W 2007 Integrated optical Ti:LiNbO3 ring resonator for rotation rate sensing *European Conf. on Integrated Optics in Conf. Proc*.
[25] Ciminelli C, Dell'Olio F, Armenise M N, Soares F M and Passenberg W 2013 High performance InP ring resonator for new generation monolithically integrated optical gyroscopes *Opt. Express* **21** 556–64
[26] 2008 Beam Prop-Rsoft User Guide, RSoft Design Group, Inc. 400 Executive Blvd. Suite 100 Ossining, NY 1056 2 http://optics.synopsys.com/rsoft/ AQ4
[27] Cantelar E, Jaque D and Lifante G 2012 Waveguide lasers based on dielectric materials *Opt. Mater.* **34** 555–71
[28] Okamoto K 2006 *Fundamentals of Optical Waveguides* 2nd edn (New York: Academic)
[29] Hutcheson L D, White I A and Burke J J 1980 Comparison of bending losses in integrated optical circuits *Opt. Lett.* **5** 276

QUERIES

Page 1
AQ1
Please specify the corresponding author and provide his/her email address.
AQ2
Please be aware that the colour figures in this article will only appear in colour in the online version. If you require colour in the printed journal and have not previously arranged it, please contact the Production Editor now.
Page 6
AQ3
Please check the details for any journal references that do not have a link as they may contain some incorrect information.
Page 7
AQ4
Please update the publication details if appropriate in reference [26].